

A Developmental Switch in Neurotransmitter Flux Enhances Synaptic Efficacy by Affecting AMPA Receptor Activation

John J. Renger, Christophe Egles,
and Guosong Liu*

RIKEN-MIT Neuroscience Research Center
Center for Learning and Memory
Department of Brain and Cognitive Sciences and
Department of Biology
Massachusetts Institute of Technology
Cambridge, Massachusetts 02139

Summary

Formation of glutamatergic synapses entails development of “silent” immature contacts into mature functional synapses. To determine how this transformation occurs, we investigated the development of neurotransmission at single synapses *in vitro*. Maturation of presynaptic function, assayed with endocytotic markers, followed accumulation of synapsin I. During this period, synaptic transmission was primarily mediated by activation of NMDA receptors, suggesting that most synapses were functionally silent. However, local glutamate application to silent synapses indicated that these synapses contained functional AMPA receptors, suggesting a possible presynaptic locus for silent transmission. Interference with presynaptic vesicle fusion by exposure to tetanus toxin reverted functional to silent transmission, implicating SNARE-mediated fusion as a determinant of the ratio of NMDA:AMPA receptor activation. This work reveals that functional maturation of synaptic transmission involves transformation of presynaptic silent secretion into mature synaptic transmitter release.

Introduction

A full understanding of the course of maturation followed by excitatory glutamatergic synapses remains an elusive goal. One of the most compelling questions to remain largely unanswered is how the physiological characteristics of mature synapses are acquired during development. Due to a combination of experimental and genetic accessibility, much of what is currently known about synapse formation and maturation has been derived from studies at the frog and *Drosophila* neuromuscular junctions (for review, see Sanes and Lichtman, 1999). However, attention has recently focused on the vertebrate central nervous system, where immature ineffectual synapses, or “silent” synapses, can develop efficacy during maturation and activity-dependent conditioning. Conversion of silent synapses into functional ones offers a powerful mechanism for mediating synaptic plasticity (for review, see Malenka and Nicoll, 1997, 1999; Constantine-Paton and Cline, 1998; Atwood and Wojtowicz, 1999; Malinow, 1999).

An elegant series of work has documented that multiple vertebrate CNS preparations harbor silent synapses

(Kullmann, 1994; Isaac et al., 1995, 1997; Liao et al., 1995; Durand et al., 1996; Wu et al., 1996; Bardoni et al., 1998; Li and Zhuo, 1998). Consistently among these preparations it has been found that immature synapses are able to undergo neurotransmitter release, but the postsynaptic responses appear to lack the α -amino-3-hydroxy-5-methyl-4-isoxazolpropionate receptor (AMPA)-mediated currents and, thus, are assumed to be ineffective at transmitting fast depolarizing signals to a postsynaptic neuron and therefore silent. The most commonly held explanation for these silent currents is the lack of functional AMPARs postsynaptically (Bernard et al., 1997; Malenka and Nicoll, 1997, 1999; Laube et al., 1998; Malinow, 1999; Petralia et al., 1999; Takumi et al., 1999; but see Kullmann et al., 1996; Kullmann and Asztely, 1998; Choi et al., 2000; Gasparini et al., 2000). Yet, a definitive demonstration that silent synapses do not contain functional AMPARs is still lacking. In fact, some apparent discrepancies in this hypothesis have been noted (for review, see Atwood and Wojtowicz, 1999). Particularly, there is disagreement between the relatively low proportion of synapses that are immunohistochemically identifiable as potentially N-methyl-D-aspartate receptor (NMDAR)-only synapses (17%–28%; Nusser et al., 1998a) and the high proportion of physiologically silent events. Use of local glutamate application to detect functional AMPAR and NMDAR receptors has shown that both types of receptors may be colocalized from early in synaptogenesis (Cottrell et al., 2000). Furthermore, a study on the assembly of individual glutamatergic synapses has shown that the time courses of AMPAR and NMDAR insertion follow similar clustering kinetics (Friedman et al., 2000). Additionally, work has shown that initial insertion and localization of glutamate receptors are independent of neuronal activity (Craig et al., 1993; Cottrell et al., 2000; Friedman et al., 2000). These data suggest that there may be alternative explanations for mechanisms underlying silent synapse observations.

Absent thus far in studies on maturation of glutamatergic synapses are experiments that directly test whether postsynaptic sites of single silent synapses contain functional AMPARs in conjunction with NMDARs and how activation of these receptors is regulated during development. Furthermore, no studies have yet tried to define the presynaptic changes that accompany the conversion of silent to functional synapses during maturation. For this reason, there is a general lack of evidence in favor of or against the possibility that presynaptic mechanisms could participate in the maturation of silent synapses. Therefore, the goal of this study was to examine the maturation of presynaptic and postsynaptic properties at glutamatergic synapses during the developmental period when silent transmission becomes functional.

Results

Synapsin I Localization Precedes Functional Dye Uptake during Synaptic Maturation

Cultured hippocampal neurons extend neurites and form synapses in a developmentally stereotypical and

*To whom correspondence should be addressed (e-mail: liu@mit.edu).

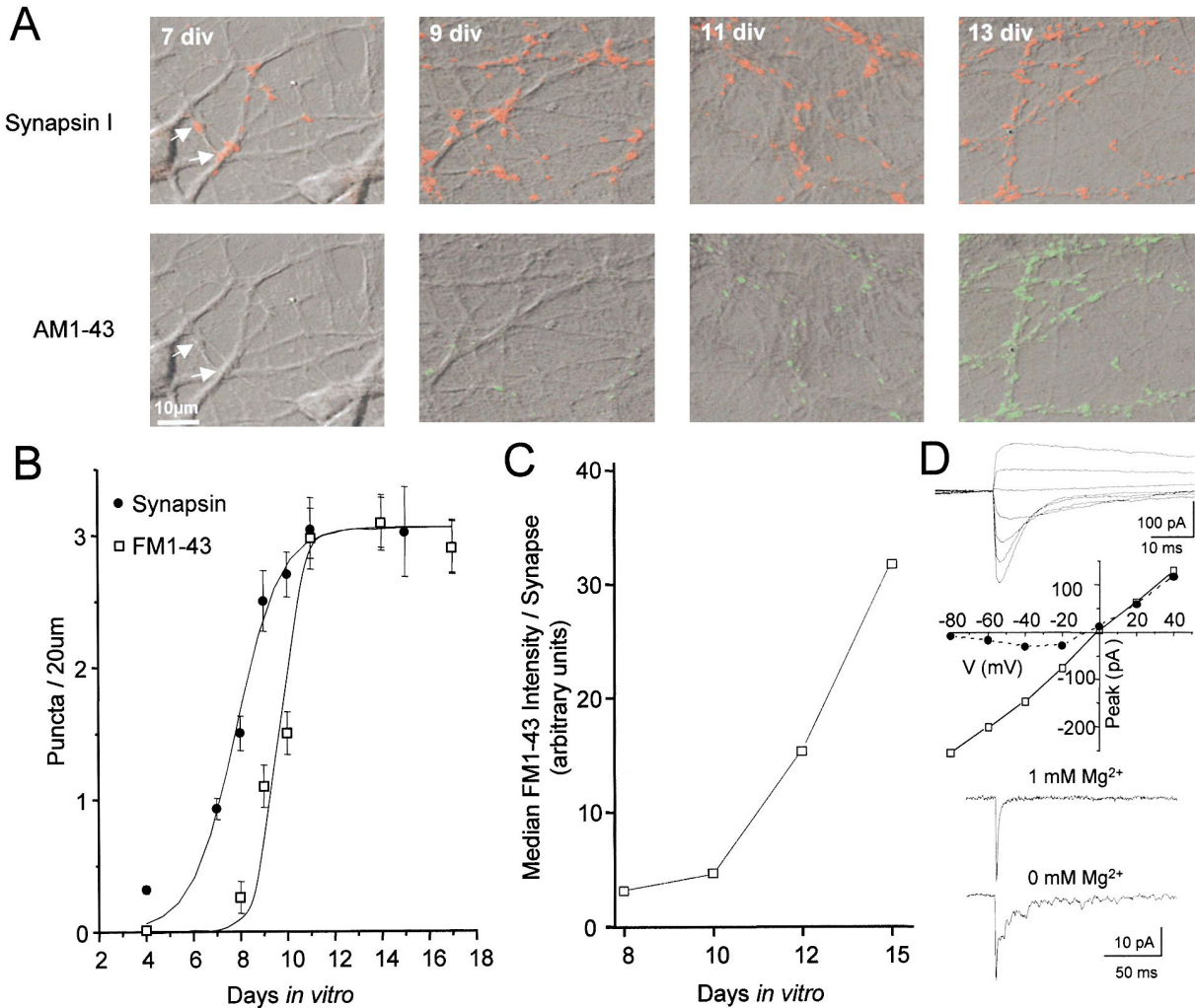


Figure 1. Functional Synaptic Vesicle Turnover follows Synapsin I Localization

(A) Cultured hippocampal terminals were functionally labeled with AM1-43 and stained for anti-synapsin I. AM1-43 (green) and anti-synapsin I (red) images were taken concurrently to directly relate functionality of putative individual presynaptic boutons with localization of synapsin I. Synapsin I puncta preceded functional labeling of synaptic terminals during development.

(B) Comparison of synapsin I puncta and FM1-43 puncta during development. Synaptic vesicle turnover followed accumulation of the presynaptic protein by a 1–2 day delay. Puncta were normalized to length of arbor to separate increases in synaptic density from possible confounding growth processes.

(C) FM1-43 intensity per punctum increased during maturation, following the initial appearance of endocytotically functional puncta (8 DIV, $n = 33,285$; 10 DIV, $n = 43,384$; 12 DIV, $n = 20,871$; and 15 DIV, $n = 62,181$).

(D) I–V relation of the typical glutamate-evoked response from single FM puncta. (Top) Representative set of iontophoretically evoked responses at graded membrane potentials. (Middle) I–V plot for the peak AMPA (filled circles) and NMDA (open squares) receptor-mediated components of the glutamate-evoked response. (Bottom) Excitatory postsynaptic currents under normal conditions (17 DIV, 1 mM external Mg²⁺; $V_h = -60$ mV) that reveal AMPAR or under conditions that allow for detection of AMPAR and NMDAR currents (0 mM external Mg²⁺; $V_h = -60$ mV).

nearly synchronous manner, providing a system well suited for studying maturational changes during synaptic development. To determine when the molecular framework for synaptic terminals is assembled in our culture system, we used a presynaptic vesicle-associated protein, synapsin I, as a developmental marker for tracking synaptogenesis (Fletcher et al., 1991). An increase in synapsin I localization to putative presynaptic terminals began at 7 days in vitro (DIV) and lasted over the next 4–5 days of development until reaching saturated levels at 11–12 DIV (Figure 1). During this period, the density of synapsin I-positive terminals in-

creased by 3-fold, representing a rapid phase of new synapse formation (0.93 ± 0.08 to 3.05 ± 0.23 puncta/20 μ m; $n = 100$ dendritic segments of 400 μ m length each). To assess the functional status of these terminals, we used a presynaptic functional marker, FM1-43 (Betz et al., 1992), and a new fixable analog of FM1-43 called AM1-43 to determine when synapsin I-positive terminals (Figure 1A, red puncta) became endocytotically competent. Unexpectedly, synapsin I-positive terminals in immature neurons were incapable of being labeled with AM1-43 (compare top and bottom in Figure 1A; 7 DIV). In contrast, as cultures neared 11–12 DIV, most synapsin

I puncta were colocalized with AM1-43 labeling (Figures 1A and 1C), suggesting that additional maturation of synapsin I-positive terminals was required before synaptic vesicles were competent to take up and retain the functional dye.

To determine whether the increased dye uptake was due to an abrupt “switching on” of synaptic vesicle recycling or if the increased uptake by synapses developed gradually, we examined the time course of dye-loading competency. Comparisons of FM1-43 intensity per labeled puncta revealed that between 8 to 10 DIV the level of dye uptake increased moderately, suggesting that, while the synaptic terminals became functionally competent, they had a low capacity for dye uptake (Figures 1B and 1C). In contrast, from 10–15 DIV, the total amount of FM1-43 per punctum increased significantly. Thus, initiation of synaptic vesicle turnover (8–10 DIV) was followed developmentally by an increased ability for dye uptake (11–15 DIV).

To confirm that puncta labeled with FM dyes are associated with the existence of postsynaptic receptors, we used iontophoretic application (100 nA; 1 ms) of glutamate to individual isolated small puncta. Indeed, functional AMPA and NMDA receptors were colocalized with labeled puncta and exhibited the typical properties of NMDA and AMPA I-V relationships observed in other preparations. Figure 1D shows a representative set of iontophoretically evoked currents and an I-V plot of AMPA and NMDA receptor-mediated currents, indicating that the functional presynaptic markers are indicative of pre- and postsynaptically functional synapses (see also Liu et al., 1999; Cottrell et al., 2000).

Maturation of Endocytotic Labeling Is Correlated with Conversion of Silent to Functional Transmission

Alterations in presynaptic function prompted the examination of how synaptic transmission might be affected during this period of development. Figure 2A displays a typical set of miniature excitatory postsynaptic currents (mEPSCs) recorded from neurons at different times of synaptic maturation. Interestingly, AMPAR-mediated mEPSCs (mEPSC_{AMPA}, which are blocked by NBQX) were almost undetectable in immature cultures (Figure 2A, top). In contrast, following removal of Mg²⁺ to detect NMDAR-mediated responses (which are blocked by APV and CPP; Hestrin et al., 1990), synaptic events comprised primarily of NMDAR-mediated currents were observed in immature cultures (Figure 2A, middle and bottom). These “AMPA-quiet” synaptic events (mEPSC_{AMPA-quiet}) were most visible in 8 DIV neurons, whereas most mEPSCs recorded from 15 DIV neurons contained both AMPAR- and NMDAR-mediated currents (mEPSC_{dual}). The observation of more mEPSC_{AMPA-quiet} events in immature neurons is consistent with findings in hippocampal slice and cultures (Durand et al., 1996; Gomperts et al., 1998; Liao et al., 1999), suggesting that synaptic transmission from immature synapses is functionally silent.

We examined the relationship between AMPAR- and NMDAR-mediated current amplitudes for individual mEPSCs. Using the intrinsic kinetic differences in the activation and deactivation of the two receptor types,

we determined the ratio of their peak amplitudes from mEPSCs recorded under 0 mM Mg²⁺ conditions. In immature neurons (8 DIV; Figure 2B), mEPSCs were primarily mediated by NMDARs. In contrast, for mature neurons (13 DIV; Figure 2B), the majority of mEPSCs contained both AMPA and NMDA components, although a small percentage of events still lacked a predominant AMPAR component. For those events containing clear dual components, their amplitudes were correlated. This correlation (Dubè and Liu, 1999; McAllister and Stevens, 2000; Watt et al., 2000) is associated with the coordinated activation of AMPARs and NMDARs under varying concentration of transmitter within the synaptic cleft. Blockade of AMPAR activation by the antagonist NBQX resulted in a shift of ratios toward a vertical slope in mature neurons but was less noticeable in immature neurons, confirming that the majority of mEPSCs recorded from immature synapses were comprised primarily of NMDAR-mediated current.

To examine whether mEPSC_{AMPA-quiet} events are indeed NMDA only or whether they contain small AMPAR-mediated currents, we compared the times to peak of mEPSC_{AMPA-quiet} events during development. Inset in Figure 2B shows the averaged time to peak for 50–60 overlaid trials of mEPSC_{AMPA-quiet} events in the presence or absence of NBQX. The rise time of mEPSCs_{AMPA-quiet} is slower after blockade of AMPARs, indicating that mEPSCs_{AMPA-quiet} contained low levels of AMPAR activation. This observation suggests that the mEPSCs_{AMPA-quiet} occurred at synapses containing mixed receptor complements, not at NMDA receptor-only synapses. Thus, it is more appropriate to refer to the predominantly NMDA receptor-mediated events as mEPSCs_{AMPA-quiet} rather than NMDA-only events.

Interestingly, it was evident that the time to peak of pure mEPSCs_{NMDA} recorded in the presence of NBQX became faster as synapses matured. The time-to-peak distribution of pure mEPSCs_{NMDA} was significantly slower in less-developed synapses as compared with distributions observed in older neurons (Figure 2C; $p < 0.0005$, Kolmogorov–Smirnov test). The developmental decrease in the time to peak of mEPSCs_{NMDA} could not be attributed to the developmental switch from NMDAR2B to NMDAR2A subtypes (Tang et al., 1999), because there were no differences in the times to peak of pure NMDAR currents evoked by iontophoretic application of glutamate onto 9 DIV and 17 DIV synapses (Figure 2C, inset). Therefore, during synaptic maturation, quantal excitatory synaptic transmission underwent two major changes: an increase in the AMPAR-mediated component and faster NMDAR activation.

Evoked Release Reveals Trial-to-Trial Fluctuations among EPSC_{AMPA-quiet} and EPSC_{dual} Transmission at Single Synapses

To better understand silent synaptic transmission, we studied quantal synaptic release at putative single synapses by direct stimulation of individual presynaptic terminals under TTX (Kirischuk et al., 1999). In this way, it was possible to directly test for the presence of NMDARs and AMPARs and to investigate how the conversion of silent contacts into functional synapses occurs at the single synapse level.

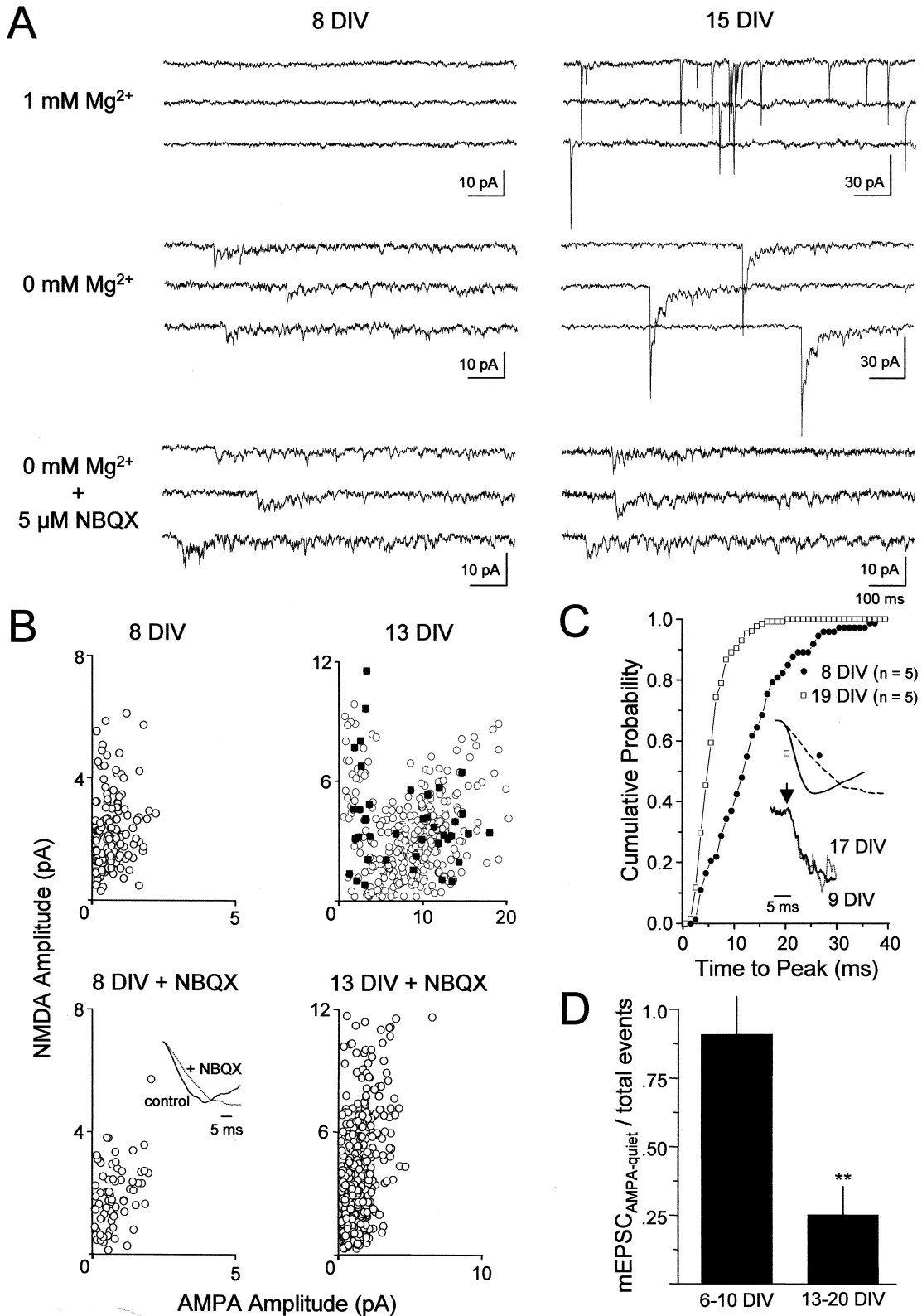


Figure 2. Comparison of mEPSCs during Development

(A) Representative examples of mEPSCs from 8 DIV and 15 DIV neurons under 1 mM Mg²⁺ (Top), 0 mM Mg²⁺ (Middle), and 0 mM Mg²⁺ with 5 μM NBQX (Bottom). Note appearance of silent or AMPA-quiet EPSCs after removal of Mg²⁺. Addition of 5 μM NBQX, an AMPAR antagonist, reveals the time course of the NMDAR-only EPSCs.

(B) Scatter plots of AMPA (with respect to NMDA) current amplitude of miniature EPSCs during synaptic maturation. In immature neurons (8 DIV), most EPSCs were comprised primarily of NMDA current. In contrast, after maturation (DIV 13), most EPSCs contained both AMPA and

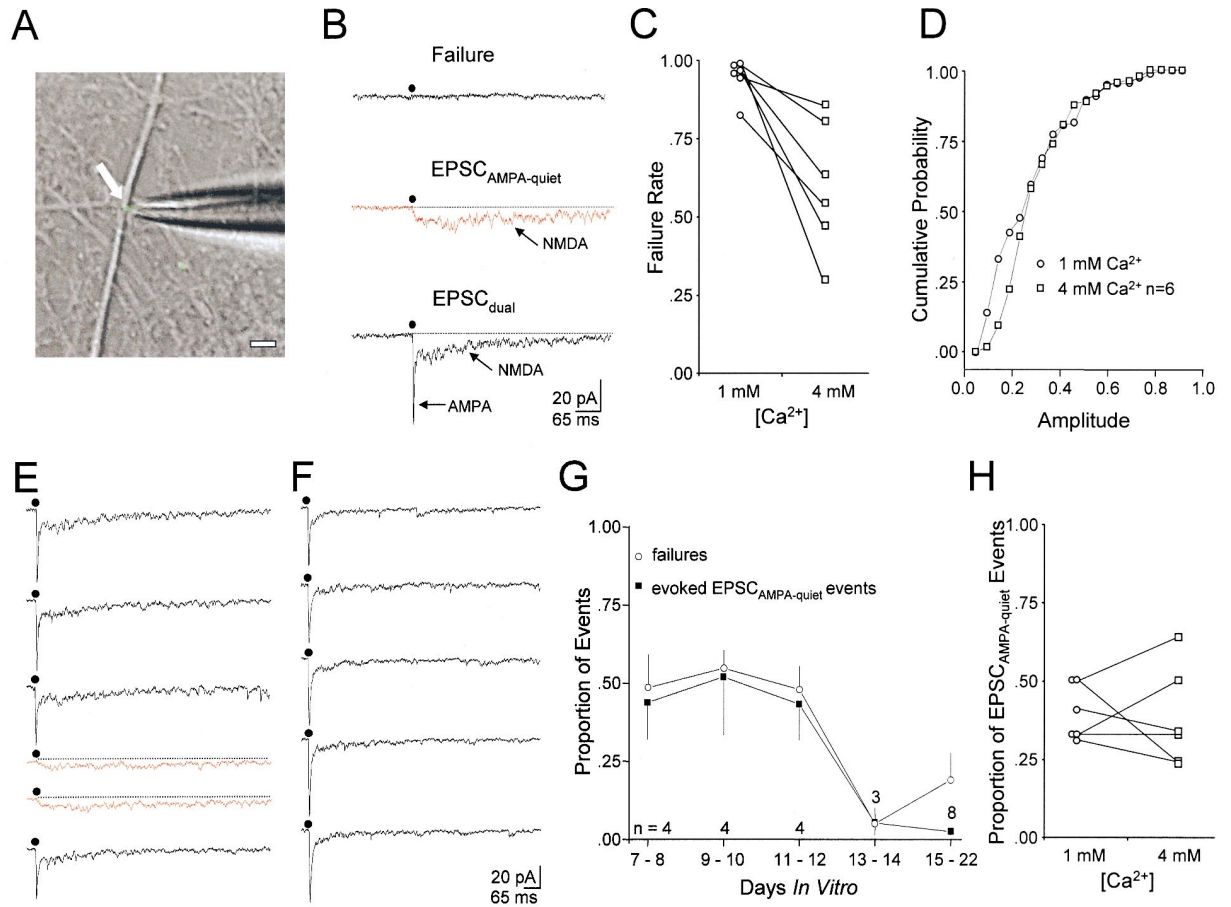


Figure 3. Evoked Synaptic Release Fluctuates among EPSC_{AMPA-quiet} and EPSC_{dual} Responses

(A) Experimental configuration for single synapse stimulation. Isolated synaptic sites with FM1-43 (arrow) were stimulated. Scale bar = 10 μm .
 (B) Representative traces demonstrating responses to focal stimulation: Failure, predominantly NMDAR-mediated response (EPSC_{AMPA-quiet}; red trace), and dual AMPAR and NMDAR response (EPSC_{dual}). Stimulus artifacts are blanked. Filled circles mark stimulus application (1 $\mu\text{A}/1$ ms).
 (C) Histogram comparing the proportion of stimulus trials that result in a failure to release neurotransmitter at differing external Ca^{2+} concentrations. Electrical stimuli applied to the same putative single synapse at low (1 mM) and high (4 mM) show the difference in the failure rates at the two Ca^{2+} concentrations. $p < 0.005$; paired Student's *t* test.
 (D) Cumulative amplitude distribution for evoked EPSCs under two external Ca^{2+} concentrations (open circles, 1 mM; open squares, 4 mM). Distributions of evoked release did not differ under reduced Ca^{2+} levels (Kolmogorov-Smirnov test). The same synaptic sites were used for both conditions (12 DIV, $n = 6$). Amplitudes were normalized to the peak amplitude of the maximal response under each condition.
 (E) Series of evoked events from a 10 DIV neuron. Note that evoked events varied between EPSC_{dual} (black traces) and EPSC_{AMPA-quiet} (red traces) responses at single synapses. Currents are shown in a successive series with failure events removed. Stimuli were applied at 0.2 Hz.
 (F) Same experimental paradigm as shown in (E) from a 14 DIV neuron. A higher proportion of evoked EPSC_{dual} events was observed.
 (G) The proportion of EPSC_{AMPA-quiet} events and the rate of synaptic transmission failures decreased over the same period of development.
 (H) The proportion of EPSC_{AMPA-quiet} events did not change with increases in Ca^{2+} concentration ($p = 0.83$), although synaptic failures were reduced significantly.
 (C, D, and H) Data were derived from the same set of experiments.

Individual presynaptic terminals were identified with FM1-43 dye labeling in conjunction with confocal microscopy. Focal electrical stimulation (1–3 μA for 1 ms)

was applied to isolated synaptic terminals. When isolated putative single synaptic sites (Figure 3A) were electrically stimulated, evoked responses could be reliably

NMDA currents, although a small percentage of EPSCs still lacked AMPAR current. Black squares represent events from a single neuron. (Inset, bottom left) Normalized traces for 50–60 aligned NMDAR mEPSCs with (dotted line) and without (solid line) NBQX. Traces demonstrate the presence of AMPAR current contamination in the rise time of apparent NMDAR-only mEPSCs.

(C) Change in rise time of mEPSC_{NMDA} during synaptic maturation. Rise times of mEPSC_{NMDA} from 8 DIV neurons were significantly slower than from 17 DIV neurons. (Inset) Upper traces are averaged events of 50–60 mEPSC_{NMDA}; lower traces are iontophoretically evoked NMDAR currents. Thus, the slower time to peak of mEPSC_{NMDA} is not due to the alteration of intrinsic properties of the NMDARs.

(D) Histogram comparing the proportion of mEPSC_{AMPA-quiet} events among developing neurons. The proportion of mEPSC_{AMPA-quiet} events becomes reduced during development. Age groupings were arbitrarily based on maturation of functional FM dye uptake (cf. Figure 1B). Bars are mean \pm SD; 6–10 DIV, $n = 8$; 13–20 DIV, $n = 10$; double asterisks, ANOVA $f(1,7) = 91.74$, $p < 0.0001$.

observed time locked to the stimulus artifact (Figures 3B–3D). We verified that the evoked EPSC events originated from single synapses by using several lines of evidence. First, to obtain evoked synaptic currents with electrical stimulation, the electrode tip needed to be within 1 μm of the FM1-43 puncta. Because FM1-43 puncta selected for stimulation had intersynapse distances larger than 5 μm , it was unlikely that evoked responses originated from multiple FM puncta. Second, previous work has shown that small, single FM1-43 puncta correspond to individual synaptic sites (Liu et al., 1999). In addition, we performed serial reconstructions of EM sections of synapses to confirm this conclusion in our culture system. Indeed, a majority of synapses reconstructed (18 of 21 reconstructed terminals, or $\sim 86\%$) contained single putative presynaptic active zones with single postsynaptic densities, and three presynaptic boutons contained dual release sites, each with a postsynaptic density. This number is slightly lower than has been reported previously under identical culture conditions (Forti et al., 1997) and is higher than previous reports from another group (Schikorski and Stevens, 1997). In 14% of terminals where two synapses exist, we can assume that both synapses have equal opportunity to undergo vesicle recycling and dye uptake; therefore, FM1-43 intensity should reflect a 2-fold increase. Previously, Liu et al. (1999) showed that the distribution of areas of FM1-43 staining contained $\sim 20\%$ of puncta, which were 2-fold larger than the median. Therefore, smaller FM-stained puncta have a higher probability to be those boutons with a single synaptic site undergoing synaptic vesicle turnover. Throughout this study, we were rigorous in our selection of small weakly stained puncta for all manipulations. Third, we compared the peak amplitude distribution of evoked EPSC_{dual} events obtained at high and low external Ca^{2+} concentrations. Since the probability of release is steeply dependent upon external Ca^{2+} concentration (Dodge and Rahamimoff, 1967), the chance of simultaneous release events overlapping from multiple release sites should be reduced significantly by decreases in external Ca^{2+} concentration. If evoked events originate from multiple synapses, their peak amplitude distribution would be expected to shift to the left under decreasing external Ca^{2+} concentrations. We used a reduction in external Ca^{2+} from 4 mM to 1 mM to reduce the probability of release at putative single synapses. This reduction in external Ca^{2+} led to a reduction in the probability of release (Figure 3C). However, it did not shift the distribution of the peak amplitudes of EPSCs (Figure 3D). Furthermore, the amplitude distribution of evoked EPSCs was not different from amplitude distributions of mEPSCs. Thus, the electrical stimulation protocol used here provided a reliable method to examine transmitter release at the single synapse level.

Focal stimulation applied under 0 mM Mg^{2+} conditions resulted in one of three types of response: (1) a failure of release, (2) a sustained low-amplitude NMDA current (EPSC_{AMPA-quiet}), or (3) a transient AMPAR-mediated current combined with the slow NMDA current (EPSC_{dual}) (Figure 3B). No AMPA-only responses were observed under 0 mM Mg^{2+} conditions during the course of these experiments. Unexpectedly, when synaptic EPSCs were electrically evoked at single immature synapses (10 DIV),

postsynaptic currents fluctuated between EPSC_{AMPA-quiet} and EPSC_{dual} (Figure 3E). In contrast, most EPSCs evoked from more developed (13–22 DIV) synapses contained both AMPAR- and NMDAR-mediated responses (Figure 3F). The occurrences of EPSC fluctuations among evoked trials were observable throughout development. To examine the time course of this conversion, we plotted the percentage of EPSC_{AMPA-quiet} responses during synaptic maturation (Figure 3G). At 7–12 DIV synapses, EPSC_{AMPA-quiet} responses were approximately half of the total evoked responses ($50\% \pm 8\%$; $n = 12$ synapses), whereas, at more mature synapses (13–22 DIV), EPSC_{AMPA-quiet} responses were rarely detectable ($2\% \pm 1\%$; $n = 11$ synapses). Young synapses were also more likely to result in a true failure of synaptic transmission than older synapses (7–12 DIV = $52\% \pm 5\%$, $n = 12$ synapses; 13–22 DIV = $5\% \pm 3\%$, $n = 11$; ANOVA, $F(1, 10) = 19.72$, $p < 0.0013$). Under normal external Mg^{2+} conditions, the failure rate for young synapses (7–12 DIV) was $\sim 75\%$ if both the true failures and the evoked events, which lack clear AMPA currents, are considered together as failures of transmission.

An apparent correlation between the failure rate and the proportion of evoked events that resulted in EPSC_{AMPA-quiet} events could be found throughout development (Figure 3E). To test whether increased probability of synaptic release and reduction of EPSC_{AMPA-quiet} events were causally related, we examined the effects of altering external Ca^{2+} on the proportion of EPSC_{AMPA-quiet} responses. The failure rate of synaptic transmission decreased after increasing the external Ca^{2+} (12 DIV; Figure 3C), but it did not alter the proportion of evoked EPSC_{AMPA-quiet} events (Figure 3H). This suggests that, although the reduced failure rate and decrease in EPSC_{AMPA-quiet} events are temporally correlated during maturation, there was not a causal relationship between the two developmental trends.

EPSC_{AMPA-quiet}/EPSC_{dual} Response Type Is Determined by the Concentration Profile of Neurotransmitter Flux

Since NMDAR-mediated current responses proved to be a reliable indicator of presynaptic transmitter release for both EPSC_{AMPA-quiet} and EPSC_{dual} events, the fluctuations between EPSC_{AMPA-quiet} and EPSC_{dual} responses might be attributed to a variation of postsynaptic AMPAR responses to presynaptic release among trials. Two possible mechanisms that could mediate this fluctuation were considered: changes in the number or properties of AMPARs between trials or changes in AMPAR activation by variation in transmitter concentration or duration.

To determine whether the variation in AMPAR-mediated responsiveness was due to a change in postsynaptic receptors, it was necessary to test the functionality of postsynaptic AMPARs at synapses undergoing EPSC_{AMPA-quiet} transmission. This was done by comparing postsynaptic responses to endogenously released transmitter and to glutamate applied by iontophoresis (Figure 4A). Figure 4C illustrates the typical results from such experiments. When electrical stimulation was applied to a synapse (open vertical bars), the responses fluctuated between failures and EPSC_{AMPA-quiet} events. However, iontophoretic application of glutamate to the

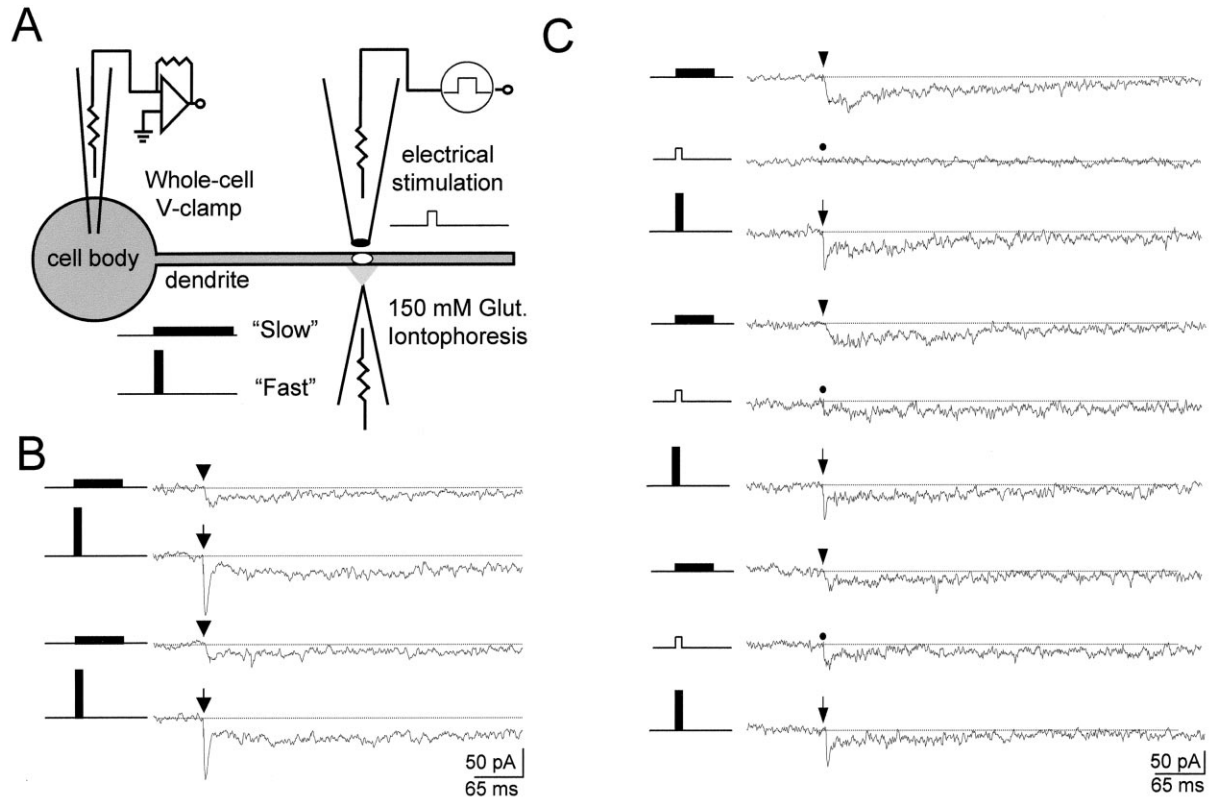


Figure 4. Concentration Profile of Neurotransmitter Delivery Determines AMPAR Activation

(A) Representation of the experimental design for concurrently stimulating presynaptic release and iontophoretically examining the postsynaptic receptors. Iontophoresis and stimulating electrodes are brought to within $1 \mu\text{m}$ of an isolated synapse. Filled vertical and horizontal bars, used throughout the figures, represent the Fast (1 ms, 100 nA) and Slow (10 ms, 10 nA) iontophoretic application parameters.

(B) AMPA receptors are not activated by a Slow flux of glutamate. Slow pulses elicited NMDAR-only responses, while Fast pulses elicited AMPAR and NMDAR responses from the same site. Because AMPAR activation was sensitive to the instantaneous changes in the concentration of neurotransmitter, AMPA-quiet responses could be generated at synapses with functional AMPARs.

(C) Silent synapses contain functional AMPARs. EPSC_{AMPA-quiet} responses, resulting from endogenous transmitter release, were evoked by presynaptic electrical stimulation at a 9 DIV synapse (open vertical bars). Evoked synaptic events were interleaved with alternating iontophoretic applications of neurotransmitter. Although EPSCs_{AMPA-quiet} were evoked presynaptically, AMPAR responses were clearly visible at this synapse during Fast iontophoretic pulses, indicating that endogenous AMPA-quiet synaptic events occurred at synapses containing functional AMPARs ($n = 4$).

same synapse (Figure 4C, closed vertical bars) evoked both AMPAR- and NMDAR-mediated currents. Iontophoretic responses varied little from trial to trial, suggesting that the number and properties of AMPAR and NMDARs remained stable among trials. These results rule out the possibility that a rapid change in the number or the properties of AMPARs was the source of the response fluctuation between trials and provide direct evidence, in addition to the NBQX experiments described above, that EPSC_{AMPA-quiet} events can occur at synapses that contain colocalized functional AMPARs and NMDARs.

If functional AMPARs are present at these synapses, why do transmitters released from presynaptic terminals, capable of activating NMDARs, fail to activate AMPARs? We analyzed the kinetic mechanisms of AMPA and NMDA receptor activation and found that AMPAR activation is largely dependent upon instantaneous concentration of transmitter, whereas NMDAR activation is determined by both peak concentration and duration of transmitter. Thus, if transmitter flux is fast,

both AMPA and NMDA receptor will activate concurrently. On the other hand, a slow concentration profile of transmitter will selectively activate NMDAR (Dubè and Liu, 1999). Figure 4B depicts the AMPAR and NMDAR responses to applications of "Fast" and "Slow" concentration profiles of neurotransmitter. A Fast concentration profile was induced by releasing glutamate through iontophoresis with a 100 nA, 1 ms pulse. A Slow concentration profile was generated by prolonging the glutamate release to 10 ms and reducing the amplitude of the iontophoretic pulse to 10 nA to keep the total amount of transmitter delivered constant. When these concentration profiles of glutamate were alternatively applied to a single synapse (Figure 4B), it was apparent that the Fast application of transmitter activated both AMPARs and NMDARs, whereas the Slow profile applications preferentially activated NMDARs and failed to evoke clear AMPAR-mediated responses. Moreover, when a Slow profile of glutamate was delivered onto synapses where presynaptic stimulation evoked EPSC_{AMPA-quiet} responses, the evoked responses were similar to endoge-

Table 1. Ultrastructural Properties of Developing Cultured Hippocampal Synapses

DIV	Quantification of Synaptic Vesicles within Presynaptic Terminals					Vesicle Diameter (nm)	Cleft Width (nm)	Active Zone Length (nm)
	Total Vesicles	<500 nm	<100 nm	Docked	Docked/Total			
6 (21)	57.4 ± 6.6	50.3 ± 6.2	5.6 ± 0.5	1.6 ± 0.3**	0.03 ± 0.07	49.5 ± 1.5	20.8 ± 0.9	463 ± 44
9 (23)	58.4 ± 4.7	49.8 ± 4.6	6.3 ± 0.4	2.3 ± 0.4*	0.04 ± 0.01	49.9 ± 1.6	19.3 ± 1.1	427 ± 21
13 (26)	64.7 ± 5.7	51.1 ± 5.1	8.7 ± 0.8	4.8 ± 0.5	0.08 ± 0.01	48.9 ± 1.6	21.7 ± 0.9	484 ± 35

Vesicle counts are based on vesicle distance from electron-dense presynaptic active zone. "Docked" refers to those vesicles that appeared to make contact with the presynaptic active zone. * $p < 0.005$; ** $p < 0.0001$; Kolgorov–Smirnov test, with 13 DIV. A minimum of 28 samples were used for vesicle diameter, cleft width, and active zone measurements. Mean ± SEM shown.

nous EPSC_{AMPA-quiet} responses (Figure 4C, horizontal filled bars).

These data provided evidence that presynaptically evoked EPSC_{AMPA-quiet} responses could occur at synaptic sites containing functional AMPA receptors. Additionally, the concentration profile, or flux, of glutamate could determine whether the synaptic responses were either EPSC_{dual} or EPSC_{AMPA-quiet} in synapses containing both functional postsynaptic NMDARs and AMPARs. Therefore, at least some silent synapses are not postsynaptically "deaf" by virtue of AMPAR absence but rather could be silent due to an altered concentration profile of transmitter detected by the postsynaptic receptors.

Synapse Maturation Is Correlated with Synaptic Vesicle Redistribution within Terminals

During development, it is possible that multiple mechanisms influence the concentration profile of glutamate that receptors detect. We considered several factors that could modify the neurotransmitter concentration profile. First, developmental changes that affect the manner in which neurotransmitter enters the cleft or diffuses across it could alter the concentration profile of transmitter detected by receptors. Second, alterations in the geometry of the synapse that increase the distance between the point of neurotransmitter release and the receptors could reduce the effective concentration profile of transmitter. To address these possibilities we examined ultrastructural characteristics of synaptic terminals during maturation.

Table 1 presents the quantification of EM ultrastructural measurements made at synaptic terminals of 6, 9, and 13 DIV neurons, representing developmental time points before, during, and after the maturation of functional synaptic vesicle turnover, respectively (Figure 1B). An excitatory synapse was defined as an asymmetric specialization comprised of a polarized accumulation of synaptic vesicles within the presynaptic terminal, an EM-dense postsynaptic density, and tight membrane apposition between the neurons (Vaughn, 1989). Examination of developing synapses at the ultrastructural level dealt with identifying parameters that might affect the effective concentration of transmitter within the cleft. Increases in the width of the synaptic cleft would increase the diffusion distance and thus reduce both the rising slope of the concentration profile as well as the peak concentration of neurotransmitter at the receptors. Alternatively, increasing the lateral distance between the site of release and the position of the receptors would increase the diffusion distance of the neurotransmitter.

However, as shown in Table 1, no significant differences in the synaptic cleft widths or diameters of synaptic vesicles were observed. Interestingly, the only significant change that was found during the ultrastructural studies was a clear redistribution of synaptic vesicles within the presynaptic terminals during development. Adopting a system for *Drosophila* synapses (Renger et al., 2000), we quantitatively compared the proportion of synaptic vesicles that appeared tightly associated with presynaptic active zones (termed "docked") to vesicles that were within 100 nm and 500 nm and to the total number of vesicles within the terminal. Significantly more membrane-associated or docked vesicles were evident at developmental periods when synaptic terminals demonstrated both endocytotic functionality (Figure 1B) and a greater frequency of mEPSC_{dual} events (Figure 2). At 13 DIV, when essentially all synapsin I-positive synapses are endocytotically functional, the mean number of docked vesicles was increased ~2- or 3-fold over the average found at immature synapses (6 DIV = 1.6 ± 0.3 vesicles, $n = 21$; 9 DIV = 2.3 ± 0.4 vesicles, $n = 23$; 13 DIV = 4.8 ± 0.5 vesicles, $n = 26$; $p < 0.0001$ for 6 versus 13 DIV and $p < 0.005$ for 9 versus 13 DIV, Kolmogorov–Smirnov test). Increased proportions of docked vesicles might facilitate vesicular turnover, allowing increased amounts of endocytotic dyes entering into the presynaptic vesicles as the synapses mature.

Perturbation of the SNARE Complex Induces EPSC_{AMPA-quiet} Events

An alternative mechanism for regulating the concentration profile of neurotransmitter would be to control the efficiency of the transmitter release process itself. This could be achieved by regulating the diffusion of transmitter from synaptic vesicles into the synaptic cleft. A possible locus for this effect is the efficacy of the fusion process. Variations in the conductance of the fusion pore could directly influence the rate of transmitter flux during exocytosis. Low pore conductance could cause prolonged transmitter release with a low concentration profile, perhaps similar to that used to preferentially activate NMDARs (Figures 4B and 4C). Furthermore, it might restrict AM/FM1-43 uptake, resulting in poor FM dye labeling at immature synapses (Figure 1).

To examine whether the efficacy of transmitter release might cause the generation of EPSC_{AMPA-quiet} responses, we attempted to perturb the protein machinery underlying the vesicle fusion process within functional synapses. We applied tetanus toxin (TeNTx), which selectively cleaves synaptobrevin (Syb), a requisite protein

component of the SNARE complex, necessary for regulated vesicle fusion (for review, Elferink and Scheller, 1993; Südhof, 1995). We first determined an approximate time course of effect for TeNTx on mature neurons (>13 DIV), using as an assay FM1-43 dye labeling of synaptic terminals at graduated time points (Figures 5A–5C). Following increased periods of TeNTx exposure, the mature synaptic terminals became less effective at sequestering the functional marker. The distribution of median intensities of FM1-43-stained puncta revealed that treated synapses became progressively weaker, suggesting that the toxin treatment acted to inhibit functional labeling. Quantification of synapses that exceeded an arbitrary minimum intensity threshold demonstrated that 80% of the synapses failed to exceed this level after 3 hr of treatment and 90% were incapable of labeling following 24 hr of treatment.

We investigated the consequences of fusion complex disruption on mature transmission by analyzing the characteristics of mEPSCs from TeNTx-treated synapses. The frequency of miniature release events (mEPSC_{dual} and mEPSC_{AMPA-quiet}) was unchanged after 3 hr of treatment but was dramatically decreased by 24 hr of treatment (Figure 5E). However, a large proportion of miniature currents were converted from mEPSC_{dual} to mEPSC_{AMPA-quiet} events, similar to mEPSC_{AMPA-quiet} events recorded from immature synapses (Figures 5D and 5E). As the rise time of mEPSC_{NMDA} from immature synapses (Figure 2C) was slow, we compared the rise time of mEPSC_{NMDA} before and after TeNTx treatment. Interestingly, the rise times of mEPSCs_{NMDA} from TeNTx-treated synapses were significantly slower than those from similarly aged control neurons (Figure 5F) but not different from those in immature neurons (8 DIV). Therefore, mEPSCs from TeNTx-treated mature neurons exhibited similar characteristics of mEPSCs from immature neurons.

At the single synapse level, focal electrical stimulation from synapses treated with TeNTx for 24 hr failed to evoke reliable synaptic responses. However, we were able to evoke synaptic release from the 1–3 hr TeNTx-treated cultures, though the failure rate in transmission was increased significantly compared to controls (control = 14.3% ± 7%, n = 11 synapses; treated = 87.1% ± 6%, n = 6 synapses; ANOVA $f(1,5) = 76.07$, $p < 0.0003$; Figure 5H). Remarkably, most evoked EPSCs lost their AMPAR-mediated responses (Figure 5I), causing a significant increase in the proportion of evoked EPSC_{AMPA-quiet} events (control = 19.9% ± 6%, n = 11 synapses; treated = 91.4% ± 6%, n = 6 synapses; ANOVA $f(1,5) = 266.2$, $p < 0.0001$; Figure 5H). Therefore, the release mechanism at these synapses behaved in a manner similar to that observed in young neurons where the majority of release events involve AMPA-quiet synaptic transmission (Figure 2B). Perturbation of the SNARE complex, which in turn influences the fusion process, can affect AMPAR activation during synaptic transmission.

TeNTx Does Not Alter the Stability, Localization, or Activity of AMPA Receptors

Although it is known that TeNTx is able to enter presynaptic terminals through an activity-dependent uptake mechanism (Hua and Charlton, 1999), it is unclear

whether TeNTx can enter the postsynaptic membrane and affect AMPAR properties or insertion. To investigate this possibility, we used brief glutamate applications to examine the activity, clustering, and stability of AMPARs at TeNTx-treated synapses.

To test whether AMPAR localization was altered by TeNTx, dendritic arbors were “mapped” for responsiveness to iontophoretic application of glutamate. Since FM1-43 uptake was significantly reduced by toxin treatment, treated cultures were labeled with doubled concentrations of FM1-43 and then visualized on extensively high gain levels with confocal microscopy. With this technique, we checked the alignment of postsynaptic receptors to presynaptic terminals and determined the maximum postsynaptic AMPAR responses from single synapses in toxin-treated neurons. As shown in Figure 6A, the largest AMPA responses were recorded when the tip of the iontophoretic electrode was aligned with the FM1-43 dye spots. Furthermore, the AMPA current amplitudes were not reduced compared to control neurons (data not shown). These data suggest that maintenance and clustering of AMPARs was not significantly affected by toxin exposure. Moreover, the AMPA and NMDA activation kinetics were unaltered by the toxin treatment, because the treated synapses responded in a manner consistent with the receptors in the untreated neurons to Fast and Slow concentration profiles of glutamate (Figure 6B).

Since immature synapses and TeNTx-treated synapses frequently fluctuated from EPSC_{dual} to EPSC_{AMPA-quiet} events, it was important to determine the level of stability of AMPARs at postsynaptic sites. Iontophoretically stimulated synapses responded stably for at least 15 min to iontophoretic applications of glutamate at 1 Hz (Figure 6C). Surprisingly, variations from trial to trial were exceedingly small and could be accounted for almost completely by the stochastic properties of channel opening. The stability of responses was consistent among synaptic sites (Figure 6D). Thus, interference with the SNARE complex did not lead to changes in the activity, localization, or properties of postsynaptic AMPARs.

Discussion

A major question in neuroscience is how synapses acquire physiological properties during maturation. Previous demonstrations that glutamatergic synapses may be conditionally silent early in development (Wall, 1977; Isaac et al., 1995, 1997; Liao et al., 1995; Durand et al., 1996; Wu et al., 1996) present the possibility that the immature nervous system may hold the potential to be dramatically sculpted through selective switching on of appropriate sets of latent connections. Therefore, understanding the recruitment mechanisms leading to transformation of silent into functional synapses may provide important insights into the establishment of the mature nervous system. We have shown that glutamatergic synapses undergo maturation in the flux of neurotransmitter entry into the synaptic cleft—a transformation that converts AMPA-quiet secretion into potent mature synaptic transmission. These findings reveal a novel form of presynaptic maturation.

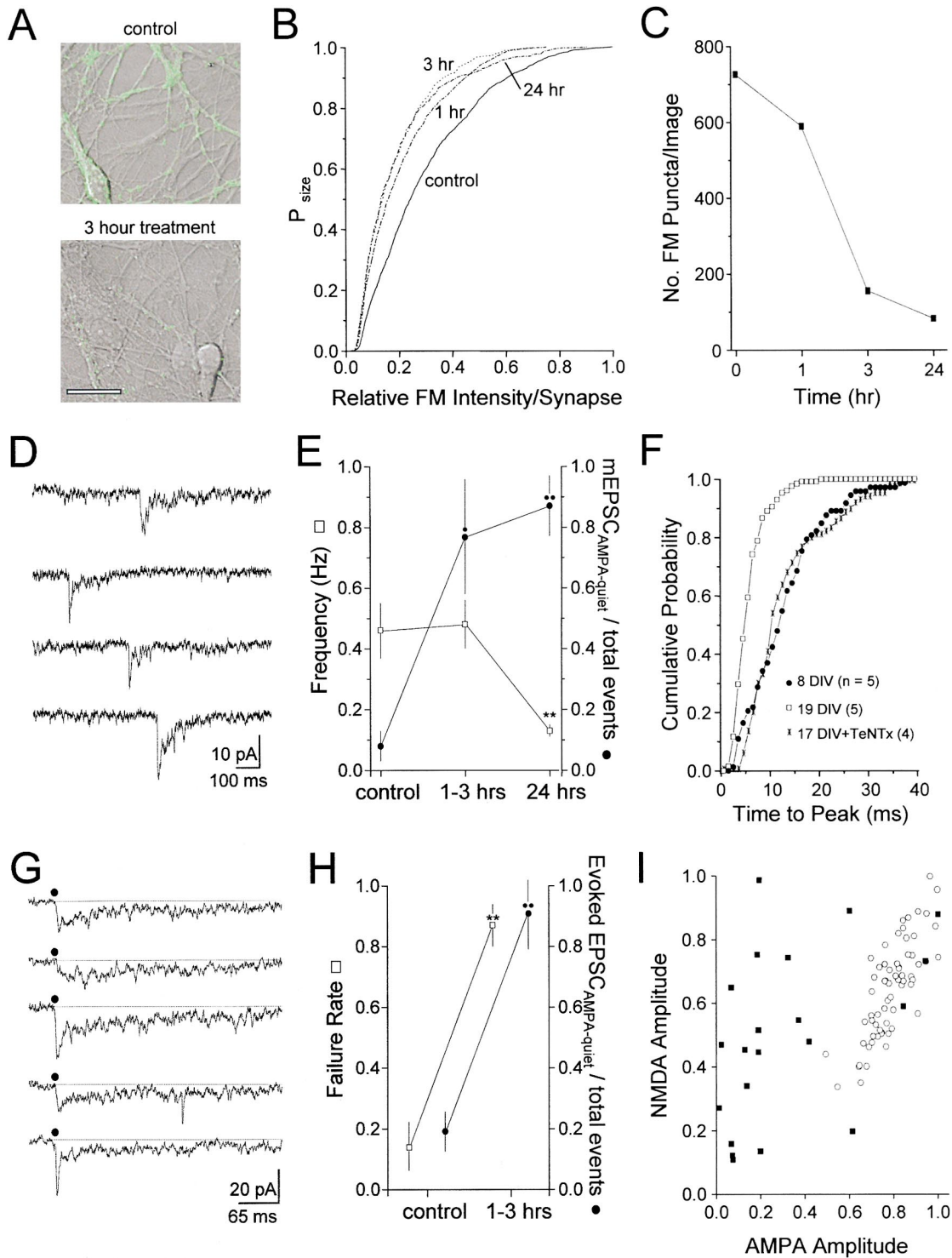


Figure 5. TeNTx Causes Reduced FM1-43 Uptake and Conversion of Functional into AMPA-Quiet Transmission

(A) Confocal images of FM1-43-loaded terminals from normal and TeNTx-treated cultures (21 DIV). Both the number of visible puncta and intensity of the puncta were reduced. Scale bar = 20 μ m.

(B) Cumulative distributions of FM1-43 dye uptake at individual synapses, normalized to the highest value under control conditions. TeNTx reduced staining intensity, indicating decreased uptake of FM1-43. The effect was maximal following 3 hr of treatment. (0 hr, n = 2177 synapses; 1 hr, n = 775; 3 hr, n = 775; 24 hr, n = 413).

(C) Comparison of FM1-43 puncta within mature neurons (13–20 DIV) treated with TeNTx. Mean number of puncta detected was reduced with exposure to TeNTx.

(D) Representative traces of mEPSCs recorded under 0 mM Mg^{2+} conditions from a 20 DIV neuron exposed for 2 hr to TeNTx.

(E) Quantitative comparison of TeNTx treatment on both miniature frequency and mEPSC_{AMPA-quiet} ratio. TeNTx treatment caused an increase

A Possible Mechanism for Silent Synaptic Transmission

In this study, we have considered the functional role of AMPA receptors in EPSC_{AMPA-quiet} transmission. During development, when the majority of miniature events are mediated predominantly by NMDA receptor-mediated current, it is possible that the postsynaptic membrane lacks functional AMPA receptors. In this experimental preparation, however, we found that silent or AMPA-quiet transmission could occur at synaptic sites containing both functional NMDA and AMPA receptors (Figures 2A–2C and 4C). Furthermore, young synapses seem to fluctuate between AMPA-quiet and functional response during evoked trials (Figure 3E). During the course of our experiments, we have considered the possibility that these phenomena are due to the highly dynamic nature of AMPA receptors versus NMDA receptors (O'Brien et al., 1998). It is possible that during synaptic transmission AMPA receptors can move in and out of the postsynaptic membrane, drift in and out of the synaptic junction, or even flip between functional and nonfunctional states. Any of these possibilities could modify the AMPA receptor response (Figure 7). These possibilities seemed unlikely to explain our observations because AMPA receptor responses to locally applied glutamate transients were highly stable among trials, even after exposure to TeNTx (Figures 4B, 4C, and 6B–6D). Furthermore, AMPA receptor activation and deactivation kinetics, clustering, and alignment with presynaptic puncta did not vary significantly from trial to trial. Therefore, it was difficult to conclude that silent or AMPA-quiet synaptic transmission events were solely due to the absence or highly dynamic nature of AMPA receptors.

Therefore, we explored alternative explanations that take into account both the immature nature of presynaptic terminals and the postsynaptic inclusion of AMPA and NMDA receptors during AMPA-quiet synaptic transmission. One possible mechanism is a change in the flux of transmitter release. We found that the activation of AMPA receptors was significantly reduced when the speed of transmitter release was slowed. However, the concentration profile of neurotransmitter did not alter the amount of NMDA receptor activation. Although there are multiple possibilities that might affect the flux of transmitter, our preferred explanation is a change in the process of vesicular fusion during synaptic transmission. If the fusion pore conductance is reduced, it would

slow the release of glutamate, and for molecules like FM1-43, which are 4-fold larger than glutamate, it could prevent passage into the vesicle. This would explain the lack of FM staining, the relatively small amount of AMPA receptor-mediated current, and the increased rise time of NMDA currents at young synapses. The perturbation of vesicle fusion through TeNTx-treatment provided a strong test of this possibility. Following toxin treatment, mature synapses generally failed to label with FM dye, had higher frequencies of miniature and evoked AMPA-quiet transmission events, higher failure rates of transmission, and slowed NMDA receptor activation, reminiscent of young synapses. To conclude that maturation of the synaptic vesicle fusion process does underlie the conversion of AMPA-quiet to functional transmission, future experiments will have to directly monitor the developmental changes in the proteins involved in the formation of the synaptic vesicle fusion complex.

It is important to note that maturation of the neurotransmitter release process, as described here, does not exclude the important role of postsynaptic receptor insertion in the development of functional glutamatergic synapses (Shi et al., 1999; for review, see Malenka and Nicoll, 1997, 1999; Malinow, 1999). During formation of early synapses, postsynaptic AMPA receptor insertion might appear after the insertion of NMDA receptors (Gomperts et al., 1998; Nusser et al., 1998b; Rao et al., 1998; Liao et al., 1999; Takumi et al., 1999; but see Friedman et al., 2000), which would generate true silent synaptic events in the presence of release from mature presynaptic terminals. Our data suggest that the addition of AMPA receptors to NMDA synapses generally occurs prior to the maturation of functional transmitter release in our culture system. Consequently, even after both receptors are present postsynaptically, synaptic transmission can still be functionally silent, possibly due to a reduced flux of transmitter from immature terminals. Work from the hippocampal slice preparation has recently suggested that presynaptic transmitter release may be involved in silent transmission (Choi et al., 2000; Gasparini et al., 2000). Understanding the regulation of both presynaptic and postsynaptic maturation will be critical for understanding the formation of functional synapses.

Neurotransmitter Flux Affects the Efficacy of Synaptic Transmission

One of the interesting findings from this work is that the concentration profile of transmitter release can dictate

mEPSC_{AMPA-quiet} events from mature terminals. Symbols are mean \pm SEM. Control, $n = 5$; 1–3 hr, $n = 4$; and 24 hr, $n = 8$ cells; double asterisks = $p < 0.0001$, Student's t test; black dot = ANOVA $f(1,3) = 81.00$, $p < 0.003$; double black dots = ANOVA $f(1,4) = 2554.4$, $p < 0.0001$; tests are with control group.

(F) Rise time of mEPSC_{NMDA} in mature neurons is slowed by TeNTx treatment. Events were recorded in NBQX. Data for 8 DIV and 19 DIV are same as Figure 2C.

(G) Representative series of evoked EPSCs from a single synapse (DIV 21) after 1 hr TeNTx treatment (0 mM Mg²⁺). Evoked EPSCs fluctuated between EPSC_{AMPA-quiet} and EPSC_{dual} among trials, reminiscent of evoked EPSCs from immature synapses (cf. Figure 3E).

(H) Quantification of EPSCs following TeNTx demonstrates that 1–3 hr exposure caused terminals to release a significantly higher ratio of EPSC_{AMPA-quiet} events and simultaneously reduced the probability of release (P_r). At 24 hr of treatment, there were no reliably evokable responses. Mean \pm SEM; control, $n = 11$; 1–3 hr, $n = 6$; double asterisks, ANOVA $f(1,5) = 76.07$, $p < 0.0003$; double black dots, ANOVA $f(1,5) = 266.2$, $p < 0.0001$; tests are with control.

(I) Relationship between AMPAR and NMDAR responses among individual EPSCs. In controls (open circles), the AMPAR and NMDAR responses were highly correlated. Following 2 hr of TeNTx, covariance is lost, inducing NMDA:AMPA ratios similar to immature EPSC_{AMPA-quiet} events (cf. Figure 2B).

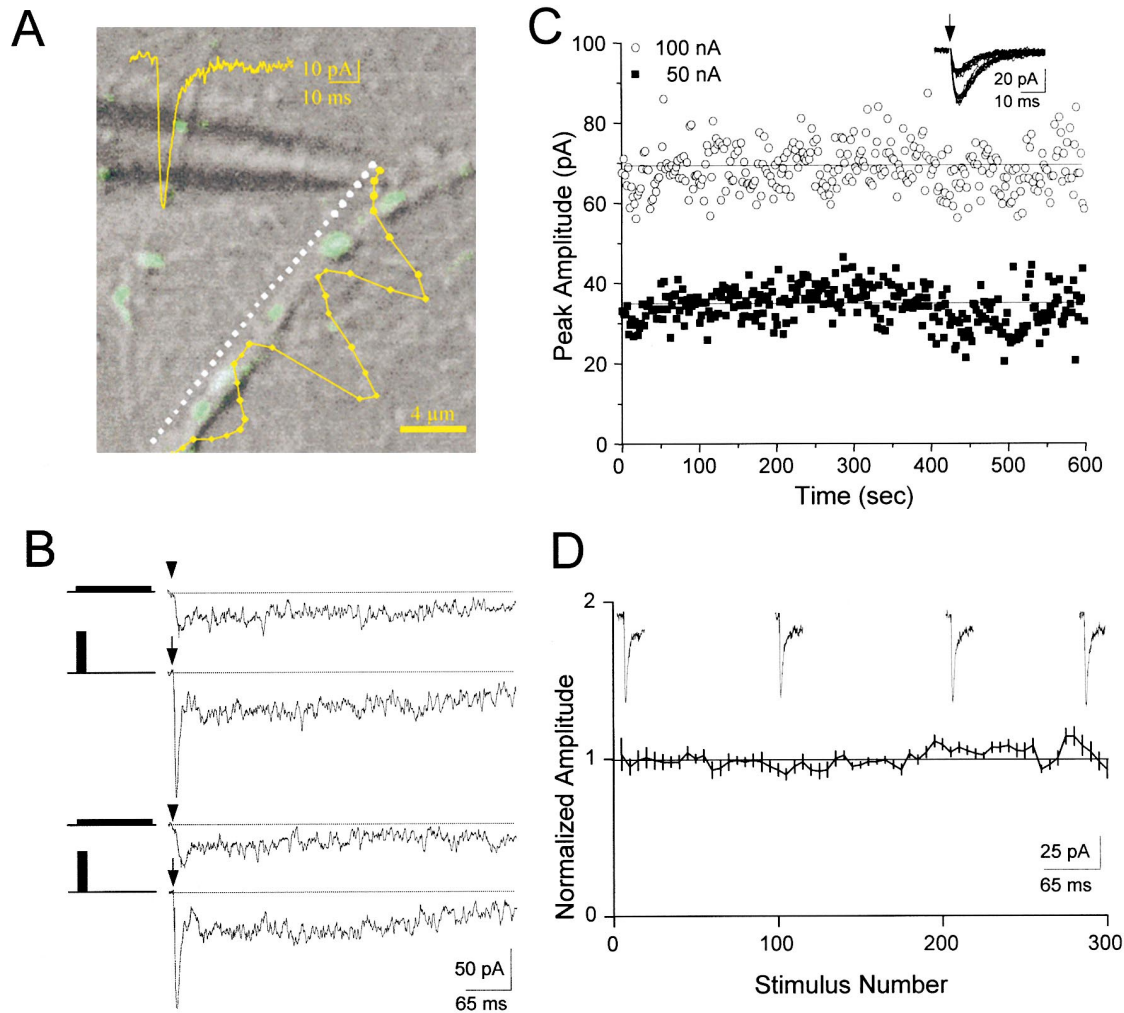


Figure 6. Postsynaptic AMPA and NMDA Receptor Properties Remain Intact following TeNTx Exposure

(A) Map of a dendritic branch of a TeNTx-treated neuron revealed functional AMPA receptors near FM-labeled puncta. Glutamate was applied at regular intervals (white dots; $0.8 \mu\text{m}$). Distance between white and yellow dot represents peak AMPA current at each location. Receptor activity and localization were similar to maps performed on controls (data not shown). Map was obtained from a 3 hr TeNTx-treated neuron. Amplitude scale bar applies to trace and map.

(B) Alternating the concentration profile of glutamate demonstrates that the activation of AMPA and NMDA receptors are unaffected following TeNTx. Example is representative of six matured synapses following 24 hr in TeNTx. Glutamate was delivered in a Fast (100 nA for 1 ms) or Slow (10 nA for 10 ms) manner.

(C) AMPARs in TeNTx-exposed synapses respond to application of neurotransmitter in a dose-dependent manner similar to untreated synapses (1 Hz; 900 trials). Stability of responses argues against rapid removal of significant numbers of functional AMPA receptors or their lateral diffusion away from synapses.

(D) Repetitive iontophoretic stimulation-induced (1 Hz) responses from TeNTx-treated neurons were averaged among synapses ($n = 4$), demonstrating the stability of the AMPA receptors. Responses were grouped (five stimulus trials) and normalized among neurons. Traces at progressive time points are shown.

the ratio of NMDA and AMPA receptor activation. It will be interesting in future work to explore the mechanisms that influence the concentration of transmitter detected by receptors. This will depend upon the amount of neurotransmitter released into the synaptic cleft and the relative distance of the receptors from the source of neurotransmitter release. Although synaptic vesicle fusion is a likely control point for determining transmitter flux, additional plausible mechanisms exist. For example, neurotransmitter buffering mechanisms and ion exchange complications between the cleft and the synaptic vesicle during release could alter the cleft concentration profile.

In contrast, misalignment of the pre- and postsynaptic structures (Uteshev and Pennefather, 1996; Xie et al., 1997) or movement of the receptors away from the presynaptic site of release would influence the effective concentration of neurotransmitter detected by the receptors (Figure 7). Therefore, it is possible that maturation of EPSC_{AMPA-quiet} into EPSC_{dual} is accompanied by a tighter registration of the presynaptic active zone and postsynaptic receptor clusters without a change in flux of neurotransmitter. In this study, we could not test all of these possibilities exhaustively. However, our data did reveal that general features such as synaptic cleft

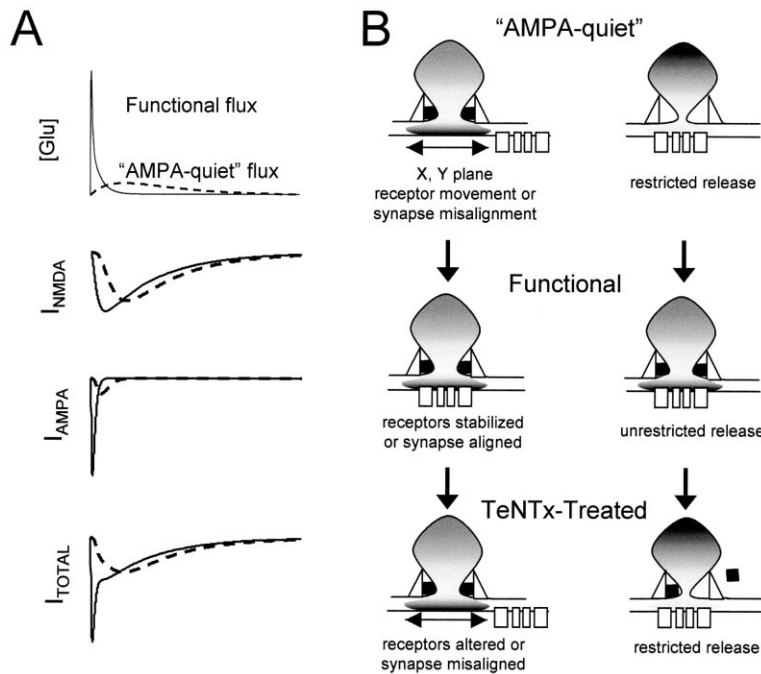


Figure 7. Maturation of Glutamate Flux Affects Receptor Activation

(A) Simulation of glutamate receptor activation in response to different transmitter fluxes. (Top) Functional (solid) and AMPA-quiet (dotted) neurotransmitter concentration profiles. The total amount of neurotransmitter is held constant. (Middle) Simulated responses of AMPA and NMDA receptors to transmitter profiles. (Bottom) Total current. Note that response to Slow flux mimics EPSC_{AMPA-quiet} responses. Traces were generated by numerical simulation of AMPA and NMDA receptor activation, under Slow and Fast concentration profiles of glutamate (see Experimental Procedures).

(B) Two hypothetical possibilities for how concentration profiles of neurotransmitter could be attained during development. (Left) During maturation, the distance between the presynaptic release site and postsynaptic receptors could be shortened to increase the effective concentration profile. This could occur by moving the receptors to a location more closely apposed to the site of release (shortening the distance in the X, Y plane of the cleft) or through altering the height of cleft (shortening the Z axis; data not shown). (Right) Alternatively, neurotransmitter concentration could be altered through controlling the diffusion of glutamate into the synaptic cleft. For example, the synaptic vesicle pore conductance may be larger during a functional than a silent or EPSC_{AMPA-quiet} event.

width, vesicle size, and the presence of pre- and post-synaptic features lacked significant differences in the developing synapses.

The central glutamatergic synapses are the only synapses of which we are aware that contain a mix of ionotropic receptors (AMPA and NMDA) to sense both the instantaneous concentration (AMPA) and the overall amount of transmitter released (NMDA). Due to the unique mix of these receptors, it is possible that these postsynaptic membranes are uniquely able to sense the concentration–duration profile of presynaptic transmitter release. It is uncertain what advantage this ability confers, although it is interesting to speculate that it may be an important mechanism for mediating plasticity at the quantal level of synaptic transmission.

Synaptobrevin Cleavage by TeNTx Induces AMPA-Quiet Transmission

It has been previously hypothesized that the fusion pore of synaptic vesicles may be a site for modification of release (for review, see Betz and Angleson, 1998). Indeed, some studies have found evidence that the synaptic vesicles may have several possible routes to follow in allowing their vesicular contents to enter the synaptic cleft, including “kiss-and-run” and full-fusion methods (Fesce et al., 1994; Henkel and Betz, 1995). However, as the volume of the synaptic vesicle is so small, it has been generally assumed that the neurotransmitter should be able to diffuse away from the synaptic vesicle within a fraction of a millisecond (Monck and Fernandez, 1994; Bruns and Jahn, 1995). In fact, synaptic transmission mediated by fast synapses, such as those found

at the neuromuscular junction (Stiles et al., 1996), glutamatergic synapses (AMPA receptor; Diamond and Jahr, 1997), and inhibitory synapses (GABA_A receptor; Galarreta and Hestrin, 1997), may reach their peak concentrations in less than 0.5 ms. These data have shown that, for mature presynaptic terminals, the size of fusion pore is not likely to restrict the diffusion of neurotransmitter. Results from numerous studies have suggested that the SNARE complex in presynaptic terminals participates in vesicle fusion (Söllner et al., 1993; Pevsner et al., 1994). The assembly of synaptobrevin, synaptotagmin, and SNAP-25 has been demonstrated to be necessary for Ca²⁺-regulated synaptic vesicle fusion (for review, see Südhof, 1995; Calakos and Scheller, 1996). Here, TeNTx has been used to specifically inactivate synaptobrevin, perturbing synaptic vesicle fusion. Appearance of EPSC_{AMPA-quiet} and slow NMDAR activation after the interruption of the SNARE complex by TeNTx suggests that the fusion conductance could become a limiting factor for transmitter release under this condition.

Implications for the Molecular Mechanisms of Synaptic Plasticity

Processes for strengthening central glutamatergic synaptic connections may take any number of forms, including insertion of postsynaptic receptors (Lüscher et al., 1999; Petralia et al., 1999; Shi et al., 1999; Takumi et al., 1999), posttranslational modifications such as phosphorylation (Barria et al., 1997), or increases in AMPA receptor single-channel conductance (Benke et al., 1998). In this report, we have presented an additional mechanism that may explain how developmental strengthening of

synaptic connections occurs. Interestingly, the transition from silent or AMPA-quiet to functional transmission is not all or none. Rather, the strength of a synaptic connection may be determined by the proportion of the synaptic events that release in a functional, high-concentration profile form, relative to the low-concentration AMPA-quiet form. The consolidation of synaptic connections may require the increased probability of mature synaptic release. Furthermore, we have found a small percentage of silent events that occur during electrical stimulation of mature synapses, suggesting that the ratio of the silent release events to functional events may be continuously regulated throughout development. The ability to transform the strength of a synapse at the level of individual EPSC events provides a fine-tuning mechanism for setting the level of synaptic efficacy, even among trials at the same synapse (Figure 3E). Further work still needs to be done to determine if activity-dependent modifications can shift the ratio of the functional and silent release events, as has been proposed by Choi et al. (2000).

One consequence of our findings is that the responsiveness of postsynaptic neurons can be modified without altering the amount of neurotransmitter that enters the synaptic cleft during synaptic transmission. This ability does not require the induction of new release sites or increases in the number of quanta released per stimulus. In fact, previous work has demonstrated that plasticity can occur without changes in the overall amount of neurotransmitter being released (Diamond et al., 1998; Linden, 1998; Luscher et al., 1998). Thus, a change in fusion efficacy, like that which we have described here, could explain how synaptic strength can be altered following plasticity, in the complete absence of any change in the total amount of neurotransmitter liberated per stimulus.

Experimental Procedures

Cell Culture and FM Dye Staining

Hippocampi were dissected from postnatal day 1–3 rat pups and cultured as previously described (Liu and Tsien, 1995). Both FM1-43 and AM1-43 staining was carried out by applying either 10 μ M N-(3-triethylammoniumpropyl)-4-(4-(dibutylamino) styryl) pyridinium dibromide (FM1-43, "synaptogreen"; Biotium, Richmond, CA) or AM1-43 (Biotium) in a solution of (in mM) NaCl, 39; KCl, 90; glucose, 30; HEPES, 25; 5 μ M D-CPP; and 10 μ M DNQX to prevent NMDA and AMPA receptor activation. AM1-43 is a form of FM1-43 with an additional aldehyde-reactive amino group at the hydrophilic end of the styryl dye, making it less sensitive to fixation. Cell cultures were fixed immediately after AM1-43 staining with 4% paraformaldehyde and permeabilized with 0.01% Triton X-100 for 15 min at 4°C. Primary antibodies against synapsin I (1/1000; American Qualex, San Clemente, CA) were applied, followed by rinses in PBS and visualized with rhodamine-conjugated secondary antibody (1/200; Sigma, St Louis, MO). FM dye labeling was imaged using a confocal microscope with an Olympus 40 \times planapochromatic water immersion lens (1.15 NA). To quantify the amount of FM uptake at single synapses, the individual FM spots were selected using ImageTool (UTHSCSA, San Antonio, TX). The average intensity and area of individual spots were calculated. The product of area and intensity was used to represent the total amount of FM uptake at an individual synapse. TeNTx (heavy and light chains; List Biological Laboratories, Inc., Campbell, CA) treatment was carried out by diluting 25 μ g toxin/250 μ l ddH₂O. Toxin was then added directly to culturing medium to reach a final concentration of 25–50 nM, after which, cultures were replaced into incubators at 37°C and 5% CO₂ until time of experiments.

Electrophysiology

Whole-cell patch-clamp recordings were performed as previously described (Liu et al., 1999). Patch pipettes (3–6 M Ω) contained (in mM) CsMeSO₃, 125; HEPES, 10; NaCl, 8; CaCl₂, 1; EGTA, 10; Mg-ATP, 2; and GTP, 0.3; pH was adjusted to 7.2 with CsOH. Extracellular solution was based on Tyrode solution (in mM): NaCl, 128; KCl, 5; glucose, 30; HEPES, 25; MgCl₂, 0.5; CaCl₂, 2.5; plus 0.5 μ M tetrodotoxin (TTX; Oretek); 10 μ M glycine (Sigma); and 50 μ M picrotoxin (Sigma); pH adjusted to 7.4 with NaOH. 1,2,3,4-Tetrahydro-6-nitro-2,3-dioxo-benzo [f] quinoxaline-7-sulfonamide (5 μ M; NBQX; Sigma) was used to specifically block AMPA currents. Access resistance was monitored online and was typically <10 M Ω . Glutamate iontophoresis (MVCS 02C Micro-iontophoresis Controller, NPI Electronics) was performed as previously described (Liu et al., 1999). High-precision micromanipulators (MP-285; Sutter Instrument Company) were used to position patch, stimulating, and iontophoresis electrodes. The position of electrodes was controlled with in-house software. Single synapse stimulation was performed similarly to the method reported by Kirischuk et al. (1999). Stimulating electrodes were pulled from single-barrel borosilicate glass and filled with extracellular solution (typical series resistances were \sim 10–12 M Ω). AMPA peak current was measured as the peak current within 3 ms following the beginning of the EPSC event, while the NMDA amplitude was defined as the average amplitude of the current measured over a 15 ms window, 20 ms after the initiation of the EPSC event. For Figures 2–7, the term "mEPSC_{AMPA-quiet}" or "EPSC_{AMPA-quiet}" describes those synaptic currents, which are composed primarily of NMDA receptor-mediated currents. Synaptic events were generally referred to as AMPA-quiet if the NMDA:AMPA ratio was greater than \sim 0.8.

Simulating AMPA/NMDA Receptor Activation with Variable Glutamate Transients

In functional synapses, the concentration of glutamate during synaptic transmission rises and decays rapidly. We use the following equation to simulate the transmitter concentration profile $A(t)$ (Clements, 1996).

$$A(t) = A_0 (1 - \exp^{-t/\tau_1}) (A_1 \exp^{-t/\tau_2} + A_2 \exp^{-t/\tau_3})$$

Where $\tau_1 = 0.2$ ms, $\tau_2 = 0.2$ ms, $\tau_3 = 1.8$ ms, $A_1 = 3.2$ mM, and $A_2 = 0.5$ mM. For AMPA-quiet synapses, our experimental results suggested that the rate of glutamate release must be reduced, causing a slower time to peak and attenuated maximum peak concentration of glutamate. However, the majority of glutamate needed to be released within 10 ms to induce the observed levels of NMDA receptor activation. Using these values as boundaries, we utilized the following equation to simulate $A(t)$.

$$A(t) = A_0 (1 - \exp^{-t/\tau_1}) \exp^{-t/\tau_2}$$

Where $\tau_1 = 7$ ms, $\tau_2 = 13$ ms, and A_0 was set so that the total amount of transmitter released under both conditions was identical. These concentration profiles and conventional kinetic models for the AMPA and NMDA receptor activation were used to simulate glutamate receptor activation.

Acknowledgments

We wish to thank Drs. Scott Waddell, Troy Littleton, Matt Wilson, Chun-Fang Wu, Xin Mu-Renger, and Susumu Tonegawa for critical reading of the manuscript, Mr. Jon Murnick and Mrs. Bing Li for providing culture assistance, Ms. Nicki Watson for EM assistance, and Vinod Rao and Lianne Habineck for help with counting miniature events. National Institutes of Health and RIKEN-MIT Neuroscience Center grants to G. L. supported this work. J. J. R. is currently a RIKEN-MIT Fellow.

Received July 27, 2000; revised December 27, 2000.

References

- Atwood, H.L., and Wojtowicz, J.M. (1999). Silent synapses in neural plasticity: current evidence. *Learn. Mem.* 6, 542–571.
- Bardoni, R., Magherini, P.C., and MacDermott, A.B. (1998). NMDA

- EPSCs at glutamatergic synapses in the spinal cord dorsal horn of the postnatal rat. *J. Neurosci.* *18*, 6558–6567.
- Barria, A., Muller, D., Derkach, V., Griffith, L.C., and Soderling, T.R. (1997). Regulatory phosphorylation of AMPA-type glutamate receptors by CaM-KII during long-term potentiation. *Science* *276*, 2042–2045.
- Benke, T.A., Luthi, A., Isaac, J.T., and Collingridge, G.L. (1998). Modulation of AMPA receptor unitary conductance by synaptic activity. *Nature* *393*, 793–797.
- Bernard, V., Somogyi, P., and Bolam, J.P. (1997). Cellular, subcellular, and subsynaptic distribution of AMPA-type glutamate receptor subunits in the neostriatum of the rat. *J. Neurosci.* *17*, 819–833.
- Betz, W.J., and Angleson, J.K. (1998). The synaptic vesicle cycle. *Annu. Rev. Physiol.* *60*, 347–363.
- Betz, W.J., Mao, F., and Bewick, G.S. (1992). Activity-dependent fluorescent staining and destaining of living vertebrate motor nerve terminals. *J. Neurosci.* *12*, 363–375.
- Bruns, D., and Jahn, R. (1995). Real-time measurement of transmitter release from single synaptic vesicles. *Nature* *377*, 62–65.
- Calakos, N., and Scheller, R.H. (1996). Synaptic vesicle biogenesis, docking, and fusion: a molecular description. *Physiol. Rev.* *76*, 1–29.
- Choi, S., Klingauf, J., and Tsien, R.W. (2000). Postfusal regulation of cleft glutamate concentration during LTP at ‘silent synapses.’ *Nat. Neurosci.* *3*, 330–336.
- Clements, J.D. (1996). Transmitter time course in the synaptic cleft: its role in central synaptic function. *Trends Neurosci.* *19*, 163–171.
- Constantine-Paton, M., and Cline, H.T. (1998). LTP and activity-dependent synaptogenesis: the more alike they are, the more different they become. *Curr. Opin. Neurobiol.* *8*, 139–148.
- Cottrell, J.R., Dubè, G.R., Egles, C., and Liu, G. (2000). Distribution, density and clustering of functional glutamate receptors before and after synaptogenesis in hippocampal neurons. *J. Neurophys.* *84*, 1573–1587.
- Craig, A.M., Blackstone, C.D., Hugarir, R.L., and Banker, G. (1993). The distribution of glutamate receptors in cultured rat hippocampal neurons: postsynaptic clustering of AMPA-selective subunits. *Neuron* *10*, 1055–1068.
- Diamond, J.S., and Jahr, C.E. (1997). Transporters buffer synaptically released glutamate on a submillisecond time scale. *J. Neurosci.* *17*, 4672–4687.
- Diamond, J.S., Bergles, D.E., and Jahr, C.E. (1998). Glutamate release monitored with astrocyte transporter currents during LTP. *Neuron* *21*, 425–433.
- Dodge, F.A., Jr., and Rahamimoff, R. (1967). Co-operative action of calcium ions in transmitter release at the neuromuscular junction. *J. Physiol.* *193*, 419–432.
- Dubè, G.R., and Liu, G. (1999). AMPA and NMDA receptors display similar affinity during rapid synaptic-like glutamate applications. *Soc. Neurosci. Abst.* *25*, 992.
- Durand, G.M., Kovalchuk, Y., and Konnerth, A. (1996). Long-term potentiation and functional synapse induction in developing hippocampus. *Nature* *381*, 71–75.
- Elferink, L.A., and Scheller, R.H. (1993). Synaptic vesicle proteins and regulated exocytosis. *J. Cell Sci. Suppl.* *17*, 75–79.
- Fesce, R., Grohovaz, F., Valtorta, F., and Meldolesi, J. (1994). Neurotransmitter release: fusion or “kiss-and-run”? *Trends Cell Biol.* *4*, 1–4.
- Fletcher, T.L., Cameron, P., De Camilli, P., and Banker, G. (1991). The distribution of synapsin I and synaptophysin in hippocampal neurons developing in culture. *J. Neurosci.* *11*, 1617–1626.
- Forti, L., Bossi, M., Bergamaschi, A., Villa, A., and Malgaroli, A. (1997). Loose-patch recordings of single quanta at individual hippocampal synapses. *Nature* *388*, 874–878.
- Friedman, V.H., Bresler, T., Garner, C.C., and Ziv, N.E. (2000). Assembly of new individual excitatory synapses: time course and temporal order of synaptic molecule recruitment. *Neuron* *27*, 57–69.
- Galarreta, M., and Hestrin, S. (1997). Properties of GABAA receptors underlying inhibitory synaptic currents in neocortical pyramidal neurons. *J. Neurosci.* *17*, 7220–7227.
- Gasparini, S., Saviane, C., Voronin, L.L., and Cherubini, E. (2000). Silent synapses in the developing hippocampus: lack of functional AMPA receptors or low probability of glutamate release? *Proc. Natl. Acad. Sci. USA* *97*, 9741–9746.
- Gomperts, S.N., Rao, A., Craig, A.M., Malenka, R.C., and Nicoll, R.A. (1998). Postsynaptically silent synapses in single neuron cultures. *Neuron* *21*, 1443–1451.
- Henkel, A.W., and Betz, W.J. (1995). Staurosporine blocks evoked release of FM1–43 but not acetylcholine from frog motor nerve terminals. *J. Neurosci.* *15*, 8246–8258.
- Hestrin, S., Perkel, D.J., Sah, P., Manabe, T., Renner, P., and Nicoll, R.A. (1990). Physiological properties of excitatory synaptic transmission in the central nervous system. *Cold Spring Harb. Symp. Quant. Biol.* *55*, 87–93.
- Hua, S.Y., and Charlton, M.P. (1999). Activity-dependent changes in partial VAMP complexes during neurotransmitter release. *Nat. Neurosci.* *2*, 1078–1083.
- Isaac, J.T., Nicoll, R.A., and Malenka, R.C. (1995). Evidence for silent synapses: implications for the expression of LTP. *Neuron* *15*, 427–434.
- Isaac, J.T., Crair, M.C., Nicoll, R.A., and Malenka, R.C. (1997). Silent synapses during development of thalamocortical inputs. *Neuron* *18*, 269–280.
- Kirischuk, S., Veselovsky, N., and Grantyn, R. (1999). Relationship between presynaptic calcium transients and postsynaptic currents at single gamma-aminobutyric acid (GABA)ergic boutons. *Proc. Natl. Acad. Sci. USA* *96*, 7520–7525.
- Kullmann, D.M. (1994). Amplitude fluctuations of dual-component EPSCs in hippocampal pyramidal cells: implications for long-term potentiation. *Neuron* *12*, 1111–1120.
- Kullmann, D.M., and Asztely, F. (1998). Extrasynaptic glutamate spill-over in the hippocampus: evidence and implications. *Trends Neurosci.* *21*, 8–14.
- Kullmann, D.M., Erdemli, G., and Asztely, F. (1996). LTP of AMPA and NMDA receptor-mediated signals: evidence for presynaptic expression and extrasynaptic glutamate spill-over. *Neuron* *17*, 461–474.
- Laube, G., Roberts, J.D., Molnar, E., and Somogyi, P. (1998). Cell type and pathway dependence of synaptic AMPA receptor number and variability in the hippocampus. *Neuron* *21*, 545–559.
- Li, P., and Zhuo, M. (1998). Silent glutamatergic synapses and nociception in mammalian spinal cord. *Nature* *393*, 695–698.
- Liao, D., Hessler, N.A., and Malinow, R. (1995). Activation of postsynaptically silent synapses during pairing-induced LTP in CA1 region of hippocampal slice. *Nature* *375*, 400–404.
- Liao, D., Zhang, X., O’Brien, R., Ehlers, M.D., and Hugarir, R.L. (1999). Regulation of morphological postsynaptic silent synapses in developing hippocampal neurons. *Nat. Neurosci.* *2*, 37–43.
- Linden, D.J. (1998). Synaptically evoked glutamate transport currents may be used to detect the expression of long-term potentiation in cerebellar culture. *J. Neurophysiol.* *79*, 3151–3156.
- Liu, G., and Tsien, R.W. (1995). Properties of synaptic transmission at single hippocampal synaptic boutons. *Nature* *375*, 404–408.
- Liu, G., Choi, S., and Tsien, R.W. (1999). Variability of neurotransmitter concentration and nonsaturation of postsynaptic AMPA receptors at synapses in hippocampal cultures and slices. *Neuron* *22*, 395–409.
- Luscher, C., Malenka, R.C., and Nicoll, R.A. (1998). Monitoring glutamate release during LTP with glial transporter currents. *Neuron* *21*, 435–441.
- Luscher, C., Xia, H., Beattie, E.C., Carroll, R.C., von Zastrow, M., Malenka, R.C., and Nicoll, R.A. (1999). Role of AMPA receptor cycling in synaptic transmission and plasticity. *Neuron* *24*, 649–658.
- Malenka, R.C., and Nicoll, R.A. (1997). Silent synapses speak up. *Neuron* *19*, 473–476.

- Malenka, R.C., and Nicoll, R.A. (1999). Long-term potentiation—a decade of progress? *Science* 285, 1870–1874.
- Malinow, R. (1999). Selective acquisition of AMPA receptors over postnatal development suggests a molecular basis for silent synapses. *Nat. Neurosci.* 2, 31–36.
- McAllister, A.K., and Stevens, C.F. (2000). Nonsaturation of AMPA and NMDA receptors at hippocampal synapses. *Proc. Natl. Acad. Sci. USA.* 97, 6173–6178.
- Monck, J.R., and Fernandez, J.M. (1994). The exocytotic fusion pore and neurotransmitter release. *Neuron* 12, 707–716.
- Nusser, Z., Lujan, R., Laube, G., Roberts, J.D., Molnar, E., and Somogyi, P. (1998a). Cell type and pathway dependence of synaptic AMPA receptor number and variability in the hippocampus. *Neuron* 21, 545–559.
- Nusser, Z., Lujan, R., O'Brien, R.J., Kamboj, S., Ehlers, M.D., Rosen, K.R., Fischbach, G.D., and Haganir, R.L. (1998b). Activity-dependent modulation of synaptic AMPA receptor accumulation. *Neuron* 21, 1067–1078.
- O'Brien, R.J., Kamboj, S., Ehlers, M.D., Rosen, K.R., Fischbach, G.D., and Haganir, R.L. (1998). Activity-dependent modulation of synaptic AMPA receptor accumulation. *Neuron* 21, 1067–1078.
- Petralia, R.S., Esteban, J.A., Wang, Y.X., Partridge, J.G., Zhao, H.M., Wenthold, R.J., and Malinow, R. (1999). Selective acquisition of AMPA receptors over postnatal development suggests a molecular basis for silent synapses. *Nature Neurosci.* 2, 31–36.
- Pevsner, J., Hsu, S.C., Braun, J.E., Calakos, N., Ting, A.E., Bennett, M.K., and Scheller, R.H. (1994). Specificity and regulation of a synaptic vesicle docking complex. *Neuron* 13, 353–361.
- Rao, A., Kim, E., Sheng, M., and Craig, A.M. (1998). Heterogeneity in the molecular composition of excitatory postsynaptic sites during development of hippocampal neurons in culture. *J. Neurosci.* 18, 1217–1229.
- Renger, J.J., Ueda, A., Atwood, H.L., Govind, C.K., and Wu, C.F. (2000). Role of cAMP cascade in synaptic stability and plasticity: ultrastructural and physiological analyses of individual synaptic boutons in *Drosophila* memory mutants. *J. Neurosci.* 20, 3980–3992.
- Sanes, J.R., and Lichtman, J.W. (1999). Development of the vertebrate neuromuscular junction. *Annu. Rev. Neurosci.* 22, 389–442.
- Schikorski, T., and Stevens, C.F. (1997). Quantitative ultrastructural analysis of hippocampal excitatory synapses. *J. Neurosci.* 17, 5858–5867.
- Shi, S.H., Hayashi, Y., Petralia, R.S., Zaman, S.H., Wenthold, R.J., Svoboda, K., and Malinow, R. (1999). Rapid spine delivery and redistribution of AMPA receptors after synaptic NMDA receptor activation. *Science* 284, 1811–1816.
- Söllner, T., Whiteheart, S.W., Brunner, M., Erdjument-Bromage, H., Geromanos, S., Tempst, P., and Rothman, J.E. (1993). SNAP receptors implicated in vesicle targeting and fusion. *Nature* 362, 318–324.
- Stiles, J.R., Van Helden, D., Bartol, T.M., Jr., Salpeter, E.E., and Salpeter, M.M. (1996). Miniature endplate current rise times less than 100 microseconds from improved dual recordings can be modeled with passive acetylcholine diffusion from a synaptic vesicle. *Proc. Natl. Acad. Sci. USA* 93, 5747–5752.
- Südhof, T.C. (1995). The synaptic vesicle cycle: a cascade of protein-protein interactions. *Nature* 375, 645–653.
- Takumi, Y., Ramirez-Leon, V., Laake, P., Rinvik, E., and Ottersen, O.P. (1999). Different modes of expression of AMPA and NMDA receptors in hippocampal synapses. *Nat. Neurosci.* 2, 618–624.
- Tang, Y.P., Shimizu, E., Dubè, G.R., Rampon, C., Kerchner, G.A., Zhuo, M., Liu, G., and Tsien, J.Z. (1999). Genetic enhancement of learning and memory in mice. *Nature* 401, 63–69.
- Uteshev, V.V., and Pennefather, P.S. (1996). A mathematical description of miniature postsynaptic current generation at central nervous system synapses. *Biophys. J.* 71, 1256–1266.
- Vaughn, J.E. (1989). Fine structure of synaptogenesis in the vertebrate central nervous system. *Synapse* 3, 255–285.
- Wall, P.D. (1977). The presence of ineffective synapses and the circumstances which unmask them. *Phil. Trans. R. Soc. London B Biol. Sci.* 278, 361–372.
- Watt, A.J., van Rossum, M.C., MacLeod, K.M., Nelson, S.B., and Turrigiano, G.G. (2000). Activity coregulates quantal AMPA and NMDA currents at neocortical synapses. *Neuron* 26, 659–670.
- Wu, G., Malinow, R., and Cline, H.T. (1996). Maturation of a central glutamatergic synapse. *Science* 274, 972–976.
- Xie, X., Liaw, J.S., Baudry, M., and Berger, T.W. (1997). Novel expression mechanism for synaptic potentiation: alignment of presynaptic release site and postsynaptic receptor. *Proc. Natl. Acad. Sci. USA* 94, 6983–6988.